Cα-Methyl-L-Valine: A Preferential Choice over α-Aminoisobutyric acid for Designing Right-Handed α-Helical Scaffolds

Journal:	*Journal of the American Chemical Society*
Manuscript ID	Draft
Manuscript Type:	Article
Date Submitted by the Author:	n/a
Complete List of Authors:	Banerjee, Raja; Maulana Abul Kalam Azad University of Technology, Department of Biotechnology and Department of Bioinformatics Sheet, Tridip; Maulana Abul Kalam Azad University of Technology, Department of Bioinformatics Banerjee , Srijan ; Maulana Abul Kalam Azad University of Technology, Department of Bioinformatics Biondi, Barbara; Institute of Biomolecular Chemistry, CNR, Padova Unit Formaggio, Fernando; University of Padova, Department of Chemical Sciences Toniolo, Claudio; University of Padova, Department of Chemical Sciences Peggion, Cristina; University of Padova, Department of Chemical Sciences

C^{α}-Methyl-L-Valine: A Preferential Choice over α-Aminoisobutyric Acid for Designing Right-Handed **α-**Helical Scaffolds

Raja Banerjee,*‡# Tridip Sheet,# Srijan Banerjee,# Barbara Biondi,† Fernando Formaggio,† Claudio Toniolo† and Cristina Peggion*†

‡Department of Biotechnology, and #Department of Bioinformatics, Maulana Abul Kalam Azad University of Technology, West Bengal (formerly known as West Bengal University of Technology), Salt Lake, Kolkata 700064, India

† Department of Chemical Sciences, University of Padova, 35131 Padova, Italy, and Institute of Biomolecular Chemistry, Padova Unit, CNR, 35131 Padova, Italy

ABSTRACT: In synthetic peptides containing Gly and coded α-amino acids, one of the most common practices to enhance their helical extent is to incorporate a large number of L-Ala residues along with non-coded, strongly foldameric α-aminoisobutyric acid (Aib) units. Earlier studies have established that Aib-based peptides, with propensity for both the 3_{10}- and α-helices, have much higher ordered 3D-structural tendency than that exhibited by their L-Ala rich counterparts. However, the achiral nature of Aib induces an inherent, equal preference for both the right- and left-handed helical conformations as found in Aib homo-peptide stretches. This property throws challenges in analysis of a model peptide helical conformation based on chirospectroscopic techniques like electronic circular dichroism (ECD), a very important tool for assigning secondary structures. To overcome such ambiguity, we have synthesized and investigated a thermally stable 14-mer peptide where each of the Aib residues of our previously designed and reported analog ABGY (where B stands for Aib) is replaced by C^{α}-methyl-L-valine (L-AMV). Analysis of the results described here from complementary ECD and ^{1}H NMR spectroscopic techniques in a variety of environments firmly establish that the L-AMV containing peptide exhibits a significantly higher preference over its Aib parent in terms of conferring α-helical character. Furthermore, being a chiral α-amino acid, L-AMV shows an intrinsic, extremely strong bias for a well specific (right-handed) screw sense. These findings emphasize the relevance of L-AMV as a more appropriate unit for the design of right-handed α-helical peptide models that may be utilized as conformationally constrained scaffolds.

INTRODUCTION

Although the tertiary and quaternary structures of proteins participate directly in function, their precise arrangements lie on the interactions and assembly of the secondary structures. Based on the predominant presence of specific backbone elements, proteins are therefore classified as "all-α", "all-β", "α/β", "α+β", and statistical coil. The 20 coded α-amino acids represent the building blocks of proteins. The legendary comment by C.B. Anfinsen [1] that in proteins the 3D-structural information is embedded within the amino acid sequence, along with statistical and experimental contemporary analyses by Chou and Fasman [2,3] and Blout and coworkers [4] indicating that individual amino acids exhibit preference for characteristic structural elements, has inspired several groups of researchers [5–10] to investigate the sequence *versus* 3D-structure relationship in proteins. The aim of those studies has been to design sequences with predefined conformational properties for future applications. Considering the propensities of individual amino acids towards a given secondary structure, a chemist can guess the probability for a particular residue to be satisfactorily utilized for the *de novo* planning of a peptide with a well characterized conformation.

To generate a functionally active peptide with a predetermined 3D-structure, one must take care of: (i) type of amino acid units; (ii) water solubility of the resulting peptides;[11,12] (iii) preserving the L-chirality; (iv) very limited expectation for alternative 3D-structures; and (v) large preference for the monomeric state.[13] In particular, L-Ala as the hydrophobic, along with L-Lys as the hydrophilic residues stand out as the most utilized, helicogenic, coded amino acids. Accordingly, they have been used to construct relatively short, right-handed helical peptides or even to design small-sized proteins that form helix bundles.[14–19] Study of such planned secondary structural elements in isolation (in a non-protein context) would provide an opportunity to

measure local *versus* global interactions aiming at identifying what makes them stable when occurring in proteins. Unfortunately, L-Ala-based, synthesized peptides in water show significant helicity only at very low temperatures.[14,17–20] As often these helical peptides at low temperatures have been used experimentally to derive the helical tendencies of other amino acids,[21] the conclusions obtained may not properly reflect those physiologically relevant.

Accordingly, to design synthetic peptides possessing a well-defined helical structure attempts have been made through incorporation of the highly helix-inducer, non-coded, $C^{\alpha,\alpha}$(*gem*)-dimethylated α-aminoisobutyric acid (Aib)[22–24] in combination with the coded amino acids.[25–32] This residue, unlike Ala, can *almost exclusively* explore regions of the ϕ, ψ backbone torsion angles of the Ramachandran plot[23,32] where both 3_{10}- and α-helices are positioned.[26,32–35] Specifically, to prepare L-Ala rich, relatively short peptides (about 10-15 residue long) that would exhibit at least moderate helicity at ambient or higher temperatures, in our previous studies[30–32] two thermostable model peptides (termed ABK and ABGY, where B stands for Aib) have been designed by insertion of multiple Aib residues. Conformational analyses with chaotropic agents (guanidinium chloride and urea)[36] have unambiguously established that the helical stability of the aforementioned L-Ala/Aib mixed peptides at ambient temperature is about twice than that shown by their related, only L-Ala based, counterparts at very low temperature.[31]

However, due to its achiral nature, Aib exhibits an equal preference for the *right*- as well as *left*-handed helices [23,32] As a consequence, for example Aib *homo*-peptide sequences can easily fold in both the enantiomeric helical states (at an equal ratio).[37–39] This property of Aib creates challenges not only in planning model peptides having helical structures with a specific screw sense, but also generates ambiguity in the analysis of the helical conformation in a generic peptide based on chirospectroscopic techniques like the extensively employed electronic circular dichroism (ECD), where the signal intensity, that provides information on the extent of the helicity, might simply arise from the difference in ellipticity of a potential diastereomeric excess. [40–43] Thus ECD, a fundamental tool for investigating peptide/protein secondary structures, especially for Ala-rich peptides where, due to resonance overlap, NMR studies are often quite difficult,[16,18,19,32] cannot offer the correct global helical content if originated from mixtures of diastereomeric right-/left-handed folds.[44]

To circumvent this and other types of uncertainties, including that arising from potentially concomitant admixtures of 3_{10}- and α-helices (the relative percentage of which is known to be principally main-chain length dependent), we have decided that a thermally stable, water soluble, appropriate model peptide is required to be designed and studied. Moreover, based on our past experience, the most convenient choice is that the three well separated (at positions 2,6, and 11, respectively) Aib residues occurring in our previously published counterpart ABGY[31,32,44] should be replaced by the extremely effective helicogenic, C^{α}-tetrasubstituted chiral C^{α}-methyl-L-valine (L-AMV), known to be characterized by a remarkable preference for the right-handed helical conformation.[45] This choice is based on a rigorous comparison with the conformational properties of the many peptides rich in amino acids methylated at the C^{α}-atom mainly investigated in the Padova laboratory over more than 30 years. The ECD spectra of the AMV peptides are remarkably intense. Available literature results for the L-AMV peptides do not report any evidence for conformations different from α- or 3_{10}-helices.[46] In particular, β-sheets or any other type of elongated secondary structures have never been authenticated experimentally. The specific, remarkable conformational rigidity of L-AMV is provided mostly by its *iso*-propyl (in addition to C^{α}-methylation) side chain with its restricted β-branching character.

In this manuscript, we are reporting the chemical characterization, and a detailed analysis of the conformational landscape of an L-AMV analog of the 14-mer ABGY peptide by use of classical spectroscopic techniques (ECD and ^{1}H NMR). To the best of our knowledge, this is one of the few published examples where L-AMV residues have been inserted in a sequence for a more appropriate design of a water soluble, thermostable, right-handed, α-helical peptide. Also, this investigation will permit for the *first time* an appropriate, *direct* comparison between the conformational tendencies of the Aib and the L-AMV residues because both have been incorporated in the *same* model peptide template.

EXPERIMENTAL PART

Synthesis, Purification, and Characterization. The crude synthetic peptide containing the three L-AMV residues incorporated in the positions (2, 6, 11) of the original 14-mer model ABGY is a (>95% purity) USV Custom Peptide Synthesis Ltd, Mumbai, India, product. This compound has been synthesized using a few changes from the well established 9-fluorenylmethyloxycarbonyl (Fmoc) solid-phase standard protocol.[47,48] In particular, due to the presence of the extremely sterically hindered AMV residues,[45,46] during each step involving them a five-time excess of the -COOH component Fmoc-amino acid has been employed, along with double coupling and extended time in a semi-automated manner to ensure completeness (checked by the Kaiser test).

Purification of the product from the final step has been performed by use of the reverse-phase HPLC technique [with a gradient of 0–60% (*v*/*v*) acetonitrile-water and a Waters 2487 instrument having a dual λ absorbance detector at 210 and 275 nm (by taking advantage from the presence in the sequence of the chromophoric C-terminal Tyr residue)]. The molecular weight (expected mass: 1415) of the single HPLC peak obtained was determined with an ESI mass spectrometer (mass obtained:1415). The HPLC

and MS Figures have been deposited in the *Supplementary Information*.

Circular Dichroism. Temperature-dependent (5–55 °C) far-UV ECD spectra of the peptide containing the three L-AMV residues in water have been recorded with a J-815 ECD-spectropolarimeter equipped with a Peltier temperature controller. Further, temperature-dependent (5–55 °C) spectra have been also measured at varying concentrations of 2,2,2-trifluoroethanol (TFE) in water (0, 10, 20 and 30% *v*/*v*), and in CH_3CN and methanol (MeOH) as well. All the TFE-related spectra have been obtained with a 2-mm path-length cuvette, while in CH_3CN and MeOH 1-mm path length has been used. The peptide concentration of the 0, 20, and 30% TFE solutions is 65 μM, while for 10% TFE it is 55 μM. For the CH_3CN and MeOH solutions, the peptide concentration is 75 μM. Our aim has been to investigate the effect of the helix-inducing solvent (TFE), as well as of the less polar aprotic (CH_3CN) and protic (MeOH) organic solvents, on the peptide conformation. ECD data have been recorded in ellipticity (θ, mdeg), while reported as mean-residue ellipticity ([θ], deg·cm^2·dmol^{-1}). Singular Value Decomposition (SVD) analysis has been carried out to obtain information on the basis spectra of the original set which will help to understand the conformational transitions. A custom script is written based on the Python programming language using the Scikit Learn library importing the module called Truncated SVD [https://scikit-learn.org/stable/modules/generated/sklearn.decomposition.TruncatedSVD.html] to compute the SVD of each set of ECD signals in different solvents. A downloadable software package called CDtoolX, developed by *Miles and Wallace* [49] on the C++ Platform is also used for generating the SVD analysis of the ECD spectral data. After normalization, the SVD plots obtained from both tools are compared and reported in the *Supplementary Information*.

Nuclear Magnetic Resonance. 1D- and 2D- ^{1}H NMR experiments [TOCSY, ROESY, and NOESY (mixing time 250 ms)], have been performed at different temperatures: (i) on a Bruker DRX 700 MHz (cryo probe) spectrometer (for fully aqueous conditions and in 20% TFE with 10% D_2O, *v*/*v*, with TSP as the internal standard) and (ii) on a Bruker Avance DRX 600 MHz spectrometer (in CD_3CN and CD_3OH with TMS as the internal standard) using standard protocols.[50] Chemical shifts of the samples (1-2 mM) are expressed in δ (ppm) relative to the respective internal standards. TOCSY experiments have been used to assign each residue, while ROESY experiments, preferred over NOESY experiments for providing clearer signals, have been useful for sequence and conformational assignments. The programs Sparky 3.113[51] and TopSpin 4.0.7 (Bruker BioSpin) have been exploited to analyze the 2D NMR data. Chemical shift assignments have been a real challenge due to spectral overlap. In particular: Gly12, Gly13, Lys4, Lys7, and Lys9 show NH chemical shifts very close (especially in organic solvents). Nonetheless, assignments are complete. Indicative long-range ROE signals have been observed. The solvents used (CD_3CN, 99.80% D; CD_3OH, 99.50% D) are Eurisotop products.

RESULTS AND DISCUSSION

Reasons for the Choice of L-AMV. Our extensive study on the conformational preferences of chiral C^α-tetrasubstituted α-amino acids, in particular about their preferred helix screw sense in peptides, has revealed that in the Cambridge Structural Database (CSD) 194 AMV residues do occur in published crystal structures.[45] Out of a total of 192 residues in di- or longer linear peptides (two are simple amino acid derivatives), 13 D-configurated AMV are found, all of them folded in a left-handed helical conformation. The remaining 179 are L-AMV, 171 of which adopting right-handed and 8 left-handed helical conformations. This statistical survey clearly indicates that, overall, all AMV residues are helical and the L-enantiomer has a predisposition to adopt the right-handed helical state to a very large extent. The average values for the backbone ϕ, ψ torsion angles of right-handed helical L-AMV residues are -54.3°, -35.8°.

Therefore, on the basis of the aforementioned largely unambiguous 3D-structural properties of the L-AMV, we have decided to incorporate it in the three, strategically located (2,6, and 11) positions of our extremely promising, terminally-blocked, 14-mer, model peptide ABGY,[31,32,44] where residues of the achiral Aib, the prototype of this α-amino acid family, have been originally introduced. The sequences ABGY and its L-AMV analog are given below. The three Lys residues are essential in imparting an acceptable water solubility to these compounds.

Amino acid sequence of the Aib-based peptide ABGY

Ac-Ala-**Aib^2**-Ala-Lys-Ala-**Aib^6**-Lys-Ala-Lys-Ala-**Aib^{11}**-Gly-Gly-Tyr-NH_2

Amino acid sequence of its L-AMV peptide analog

Ac-Ala-**L-AMV^2**-Ala-Lys-Ala-**L-AMV^6**-Lys-Ala-Lys-Ala- **L-AMV^{11}**-Gly-Gly-Tyr-NH_2

(in both sequences Ac stands for acetyl, the N^α-blocking group).

ECD Spectra in Helical Peptides and Relevant Parameters. The secondary structures of peptides are responsible for the 3D-disposition of the backbone amide moieties. In the solution state, these chromophores are typically characterized by ECD spectroscopy. In the far-UV region the ECD signature of a right-handed helical structure shows two intense negative bands (at 222 and 208 nm), arising from the $n \rightarrow \pi^*$ and parallel $\pi \rightarrow \pi^*$ excitations of the peptide chromophore, respectively, accompanied by a positive band at about 192 nm, originated from the perpendicular $\pi \rightarrow \pi^*$ excitation. The

positive band exhibits a significantly higher intensity than those of the negative bands. Thus, for a fully developed, right-handed α-helix the intensity ratios are R_2, $[\theta]_{222}/[\theta]_{208}$, ≈1 and R_1, $[\theta]_{192}/[\theta]_{208}$, ≈2. These two informative parameters can be utilized to distinguish the α-helix from the other canonical 3_{10}-helix.[40,44]

Solvent- and Temperature-Dependent ECD Spectra of the L-AMV Peptide Analog. Figure 1 illustrates the temperature dependent far-UV ECD spectra of the L-AMV containing ABGY peptide analog as a function of solvent (H_2O, TFE, CH_3CN, and MeOH). The noise-free clear spectra in the wavelength range of 250-185 nm strongly suggest the remarkable homogeneous nature of the peptide sample under investigation. In all solvents examined, appearance of two distinct negative (>200 nm) and one positive (<200 nm) (except in MeOH where the curves can be only taken to 200 nm) ECD maxima, indicates that under all experimental conditions examined the L-AMV peptide analog exhibits the typical signature of a right-handed helical screw sense. In TFE-water mixtures, upon increasing the TFE concentration (0 → 30%) the ECD curves point towards a significant enhancement of the mean-residue ellipticity, $[\theta]$, for all three ECD maxima.

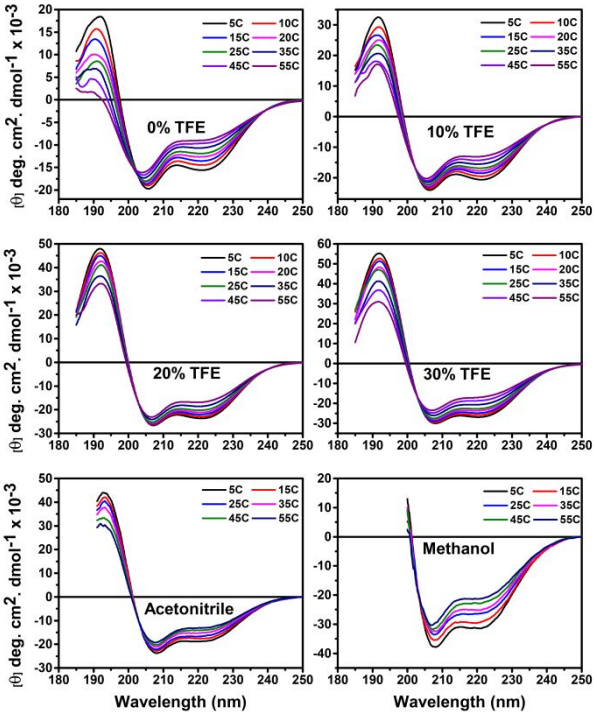

Figure 1. Far-UV ECD spectra of the L-AMV peptide analog in aqueous solution at varying (0, 10, 20, and 30%) concentrations of TFE, in CH_3CN, and in MeOH at different temperatures (5→55°C).

The representative $[\theta]_{222}$ values for the L-AMV peptide analog as a function of increasing TFE concentrations in aqueous solution between 5 and 55°C are reported in Figure 1. Interestingly, if one takes into consideration the $[\theta]_{222}\cdot10^{-3}$ (deg·cm²·dmol⁻¹) value of the negative maximum (-12.5) for its Aib-containing ABGY peptide counterpart (at 30% TFE at 5°C),[44] it turns out that it is clearly much lower in absolute magnitude than the corresponding one (-26.8) seen for the L-AMV peptide analog under the same conditions. Moreover, the magnitude of this negative maximum of ABGY is also lower than that observed for its L-AMV peptide analog (-15.5) even at 0% TFE at 5°C. This comparison clearly establishes the conclusion of an enhancement of helicity (negative ellipticity), especially that of the right-handed screw sense, upon incorporation of the L-AMV residues into the peptide. Furthermore, increase of the $[\theta]_{222}$ value with the augmentation in TFE concentration at each particular temperature strongly emphasizes that TFE promotes stabilization of the L-AMV analog helical conformation similarly to the published observation on the ABGY peptide.[44] It is worth mentioning that at 30% TFE the EDC signal intensity $[\theta]_{222}$ at 5°C reaches the maximum value for both peptides and that there would not be any significant increase in intensity upon further addition of TFE (data not shown). Such an augmentation of the overall helical structure of the peptide may occur through strengthening of the C=O···H-N intramolecular H-bonds by desolvation of the backbone upon addition of TFE *via* participation of non-helical residues, along with a stabilization of the existing helical stretch[31,32,44] of the L-AMV peptide conformation as found in water. With the increase in temperature from 5 to 55°C at a particular TFE concentration, we have observed a marked decrease in the negative intensity of the bands (both at 222 and 208 nm, especially large at 222 nm) along with a similar decrease in the positive intensity found at 192 nm. In any case, there remains a significant negative intensity at 222 and 208 nm (-9.0·10⁻³ and -12.6 ·10⁻³ deg.cm².dmol⁻¹, respectively) even at 0% TFE and 55°C, which is even higher in magnitude than that obtained for ABGY in 15%TFE at 5°C. These findings point towards a partial thermal disruption of the helical backbone of the peptide but, since it still retains a substantial helicity even at 55°C, one is allowed to conclude that the insertion of the L-AMV residues favors a highly thermostable helix for this analog.

Analogous observations on temperature-dependent ECD spectra and comparable in magnitude of ECD signal intensities at 222 and 208 nm with respect to those obtained in 0-10% TFE are recorded for the L-AMV peptide analog in both the organic solvents examined, namely CH_3CN and MeOH (Figure 1). Existence of significant helicity at high temperature (55°C) in all sorts of solvents examined confirms that the helicity in this peptide is an intrinsic pivotal property of its backbone sequence, as mentioned by Anfinsen,[1] where nature of solvent and temperature cannot play the decisive role. This finding can be considered as being due to the conformational rigidity of L-AMV residue which forces the sequence to deep into the strong helical potential well in the energy landscape. Moreover, during the partial

thermal disruption of the helical structure in all solvents, the onset of a single isodichroic point (at approximately 202 nm) (Figure 1) clearly suggests that there exists an equilibrium between two conformational states. Appearance of a single isodichroic point in temperature-dependent ECD spectra in peptides based on coded amino acids (*e.g.*, Ala) only,[30] has been usually interpreted in terms of a two-state *helix-coil* transition. However, the occurrence of an appreciable helical content (as suggested by the shape of the ECD spectra in Figure 1) even at the highest temperature examined (55°C) and in 0% TFE (100% aqueous solution) emphasizes that in the observed equilibrium there could be an involvement of two *helical states* (*e.g.*, α- and 3_{10}-helical conformations, or the co-existence of two different types of helical stretches in the same molecule which cannot be unambiguously determined from the ECD intensities).

Calculation of the Fractional Helical Content (f_H) from the Experimental $[\theta]_{222}$ ECD Value. The mean-residue ellipticity value $[\theta]_{222}$, obtained from measurements of the ECD spectra, is the parameter usually taken into consideration for calculation of the fractional helicity (f_H) of each peptide conformational state. In fact, it may provide a quantitative estimation of the helicity of peptides. Although short peptides tend to exist as conformational mixtures, the aforementioned appearance of a single isodichroic point for this L-AMV containing 14-mer peptide under all experimental conditions investigated highlights a transition between two states, where the limiting value of the 100% helical state, $[\theta_H]_{222}$, can be calculated from 43,000·(1-x/n), where n is the number of residues in the peptide and x is typically taken as 2.5 at 222 nm.[14] From the N-terminus of this peptide, a contribution of maximum 12 residues (n) would be considered as helical, due to the presence of two helix-breaking Gly residues near the C-terminus which force the final -Tyr-NH_2 moiety out of the restricted ordered conformation. A simple calculation makes $[\theta_H]_{222}$=34,000 deg cm^2 dmol^{-1}. Therefore, Eq. 1,

$$f_H = \frac{[\theta_{obs}]_{222} - [\theta_C]_{222}}{[\theta_H]_{222} - [\theta_C]_{222}} \quad (1)$$

considering the limiting value for the non-helical (*statistical coil*) state $[\theta_c]$≈0, yields

f_H at 5°C: 0.46 (0% TFE); 0.61 (10% TFE); 0.70 (20% TFE) and 0.80 (30% TFE), while f_H at 55°C: 0.27 (0% TFE); 0.38 (10% TFE); 0.46 (20% TFE) and 0.50 (30% TFE) which is much higher in magnitude than that obtained for ABGY.[32,44]

Furthermore, in CH_3CN, the calculated fractional helicity f_H is: 0.56 (at 5°C) and 0.38 (at 55°C), while in the other organic solvent studied (MeOH) it is remarkably higher: 0.92 (at 5°C) and 0.62 (at 55°C).

These f_H values, computed from the experimental $[\theta]_{222}$ data, clearly establish that incorporation of the three L-AMV residues provide exceptionally high helicity in the Ala-based peptide even if compared to its analog ABGY, reinforced by three Aib residues in the same positions of the sequence, as reported earlier.[32,44]

Utilization of the R_1 and R_2 Ratios for the Measurement of Helicity. The mean-residue ellipticity [θ] and the f_H parameter (obtained from the $[\theta]_{222}$ value) are able to provide the exact quantitative picture of helicity. However, to establish the nature of the helical structure (whether α- or 3_{10}-) of peptide molecules, the best option would be the utilization of the ratiometric ellipticity components R_1: $[\theta]_{\pi\pi^*\perp}/[\theta]_{\pi\pi^*//}=[\theta]_{192}/[\theta]_{208}$ and R_2: $[\theta]_{n\pi^*}/[\theta]_{\pi\pi^*//}=[\theta]_{221}/[\theta]_{208}$, originally proposed by Manning and Woody[40] about 30 years ago. According to their theoretical calculations,[40] the limiting values of R_2 for α- and 3_{10}-helices would be >0.8 and ~0.4, respectively, while R_1 for the α-helix would be ≈ -2 and for the 3_{10}-helix much less negative than -2. Till date, only a few attempts have been reported to characterize these two types of peptide helical structure (by use of the ratio R_2).[43,52–56] Very recently, based on the experimental evidence, for the first time it has been suggested by Banerjee and Sheet[44] that the ratio R_1 can play a decisive role in the characterization of peptide helices (for the ABGY peptide analog, R_1 for α- and 3_{10}-helices would be ~ -1.8 and ~ -1.2, respectively).

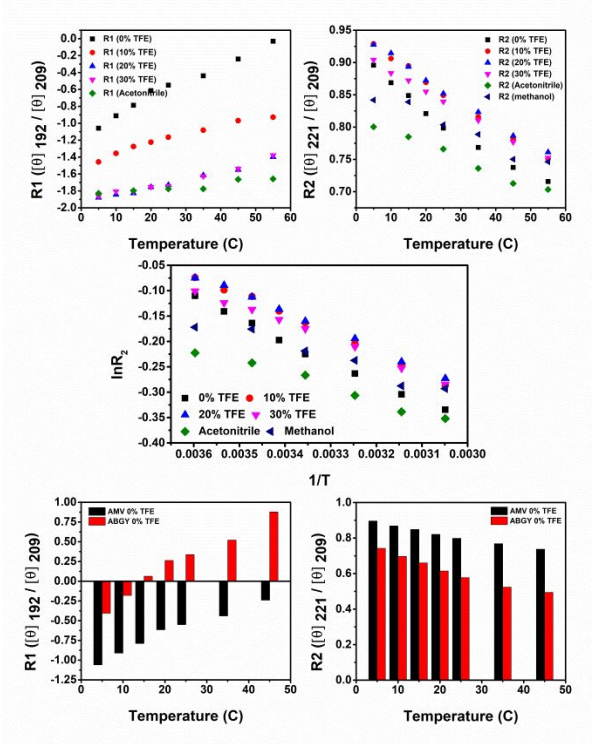

Figure 2. (Top) Plots of the R_1 and R_2 ratios for the L-AMV peptide analog in different solutions (0, 10, 20, 30% TFE, CH_3CN and MeOH) as a function of temperature in the 5° to 55°C range. (Centre) Linear dependence of lnR_2 with respect to 1/T (van't-Hoff plot).(Bottom) Histograms of the R_1 and R_2 ratios for the L-AMV and ABGY peptide analogs in aqueous solution (0% TFE) as a function of temperature in the 5° to 45°C range.

Figure 2 shows the plots of the R_1 and R_2 ratios for the L-AMV peptide analog under the different environments examined (water, aqueous TFE, CH_3CN, and MeOH as a function of temperature (5→55°C). Figure 2 also illustrates a comparison between the histograms of the R_1 and R_2 ratios for the two L-AMV and ABGY peptide analogs in aqueous solution upon increasing the temperature from 5 to 45°C.

The detailed scenario (Figure 2) of solvent- (0 to 30%TFE) and temperature-dependent R_2 values, ranging from 0.93 (5°C, 20%TFE) to 0.71 (55°C, 0%TFE), and R_1 values, ranging from -1.88 (5°C, 20%TFE) to -0.13 (55°C, 0%TFE), clearly establishes that the L-AMV peptide analog is biased to adopt a helical conformation, the nature of which is predominantly α even at higher temperatures and lower TFE concentrations. However, under fully aqueous conditions (0% TFE), although R_2 ranges from ≈0.90 (5°C) to 0.71 (55°C), indicative of highly populated α-helical state, the R_1 value, ranging from ≈1.10 (5°C) to -0.13 (55°C), is skew, not providing unambiguous support to the aforementioned conformational conclusion. However, this effect may be due to dipole-dipole interactions between the polar water and the π-π* (both perpendicular and parallel) transitions of the peptide.

The linear dependence of R_1 and R_2 with respect to temperature under each condition examined (Figure 2) also confirms the two-state transition. Furthermore, the linear dependence of $\ln R_2$ with respect to 1/T (van't-Hoff plot) (Figure 2, center) clearly indicates that in the range of the experimental temperatures considered the process of thermal helix disruption is enthalpy independent.

Not surprisingly, an in-depth comparison of the R_1 and R_2 ratios (Figure 2) between the peptide analog incorporating three L-configurated AMV residues (L-AMV) with its counterpart characterized by three achiral Aib residues (ABGY) remarkably emphasizes that insertion of the AMV residues of L-chirality into the backbone induces an extremely efficient bias towards the right-handed screw sense. Finally, the relatively lower values of the $[\theta]_{222}$ ellipticity and of the related fractional helicity (f_H) in the organic solvent CH_3CN (see above) are overruled by the magnitude of the R_2, and particularly by that of the R_1 ratio (Figure 2), which clearly point to a largely predominant occurrence of the α-helical conformation.[44]

Deconvolution of the ECD Data for Conformational Transitions. Deconvolution of solvent- and temperature-dependent ECD spectra can be employed to study two-state statistical transitions. SVD analysis of the temperature-dependent ECD spectra of the L-AMV peptide analog under all solvent conditions investigated (Figure in *Supporting Information*) has been performed using two methods, based on the Python programming language *via* the Scikit Learn library (A) and on the software package CDtoolX (B) to identify the basis spectra that would help to understand the conformational transition pathways. Under all experimental conditions examined, whether aqueous or fully organic, by use of both methods, our SVD analysis generates two components: SVD 1, which has the spectral signature characteristic of a right-handed α-helix, and SVD 2, which resembles a statistical coil curve. Overall, these results are indicative of typical helix-to-statistical coil transitions. Not unexpectedly, depending on the nature of the solvent, the limiting [θ] value varies. Nevertheless, calculations of R_1 and R_2 for SVD1 and SVD2, respectively, undoubtedly point to a transition between two states involving the α-helix and the statistical coil conformation [for SVD1: R_1 ranging from -0.69 in water to -1.75 in CH_3CN and R_2 ranging from 0.76 in CH_3CN to 0.86 in 20%TFE, while for SVD2: R_1 ranging from -0.23 in CH_3CN to 1.8 in water and R_2 ranging from 0.29 in water to -1.53 in MeOH]. Taken together, these ECD findings well justify our conclusive observation about the largely predominant 3D-structural manifestation of the α-helix upon inclusion in this peptide analog of the three L-AMV residues.

^{1}H NMR Spectra: Chemical Shifts and $^3J_{N\alpha}$ Values. The L-AMV containing ABGY peptide analog has been studied by ^{1}H NMR under different conditions of solvent (in fully aqueous conditions as well as in 20% TFE) and temperature (from 5 to 50 °C) to investigate its conformational transitions at the residue level, as ECD spectroscopy can indeed describe those changes but only on an average basis. The NH and the H^α chemical shift values of each residue have been measured from the respective TOCSY experiments. The Chemical Shift Index (CSI), which measures the directional deviation of the observed H^α chemical shift values from the respective random coil (rc) values, can provide information about the secondary structure of a peptide.[57,58]

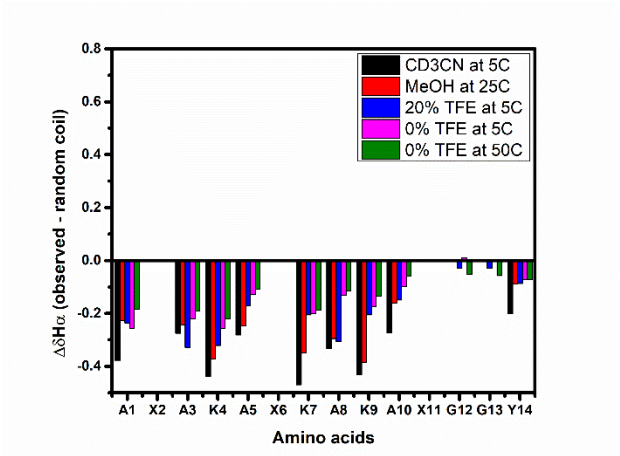

Figure 3. Chemical Shift Index (CSI) of the 14-mer L-AMV peptide in different solvent and temperature conditions.

The L-AMV peptide *under fully aqueous conditions (0% TFE)*, at both low and high temperatures (5 and 50 °C), exists predominantly in a helical conformation as judged by the criterion of the observed upfield chemical shift by > 0.1 ppm from the respective rc values (negative CSI) of

four contiguous H^{α} protons (Figure 3). Although the negative deviation is higher at low temperature compared to that at high temperature (lowering of the negative magnitude at 50 °C with respect to that at 5 °C), the difference in magnitude is not so significant as that observed for its ABGY analog. This finding indicates indeed a higher helical preference at low temperature, but the overall substantial negative CSI even at high temperatures strongly emphasizes the adoption of a thermally stable helical signature by the amino acid sequence. Although the average value of $\Delta\delta$ H^{α} for a helical backbone in proteins is ~ -0.35 ppm,[57] the comparatively smaller absolute deviations, which are increasingly smaller in its ABGY analog, could be explained owing to the presence of a statistical coil state existing in equilibrium (appearance of two states in the SVD analysis of the ECD spectra) with the helical conformer and to the solvent-exposed nature of the short monomeric helix.[59] The absolute deviations for the H^{α} chemical shift values (negative CSI) are similar (slightly higher) when the L-AMV peptide is dissolved in 20% TFE as compared to those in its fully aqueous state (0% TFE) at 5°C (Figure 3). From the comparable CSI values at 0% and 20% TFE, it could be concluded that, unlike Aib, the inclusion of the L-AMV residues in the sequence of the analog induces a strong preference for the helical backbone even in the absence of a helicogenic solvent like TFE.

This observation can be further supported by measuring the $^3J_{N\alpha}$ values (average values for the α-helix: 4.8 Hz; for the 3_{10}-helix: 5.6 Hz; for the β-strand:8.5 Hz) as this comparison offers a valuable information about the backbone torsion angle ϕ for individual residues.[60] Although for short helical peptides an averaging of the $^3J_{N\alpha}$ values would be expected due to an ensemble of conformational microstates, the temperature dependent measurements of the $^3J_{N\alpha}$ values show that at 5 °C for Ala1 to Ala10 they are found in the range ≤5Hz, while at 50 °C in the range ≤6Hz. A moderate increase in the $^3J_{N\alpha}$ values (within the range typical of the helical state) upon warming may reveal helix disruption. However, the observed magnitude clearly justifies the overwhelming existence of the helical conformation for the L-AMV containing peptide in a wide interval of temperatures, as observed from the ECD spectra and their SVD analysis.

Upfield chemical shifts of H^{α} by > 0.1 ppm from the respective rc values (negative CSI) are found throughout the sequence of the L-AMV peptide also in different organic solvents (CH_3CN at 5 °C and MeOH at 25 °C), as observed in aqueous conditions (Figure 3). The magnitude of the absolute deviation (≥ ~0.3 ppm) for the H^{α} chemical shift values is similar, especially in MeOH, when compared to that observed in 20% TFE (5°C). This result undoubtedly validates the observed ratiometric ellipticities (R_1 and R_2) and the calculated fractional helicity f_H obtained from the ECD experiments and strongly points to the onset of the helical conformation for the L-AMV peptide in all investigated environments.

A further proof for the occurrence of the helical structure could be obtained from the measured $^3J_{N\alpha}$ values. However, due to an extensive spectral overlap, a unambiguous measurement of the $^3J_{N\alpha}$ values for all of the residues is not feasible. Nevertheless, in MeOH at 25°C it still ranges near ~4.5Hz, and in CD_3CN at 5°C at ≤6Hz for the few residues for which the $^3J_{N\alpha}$ values could be measured.

^{1}H NMR Spectra: Solvent Exposure of Amide NH Protons. The nature of a helix, whether α- or 3_{10}-, can be substantiated by the number of solvent-exposed amide NH protons at the N-terminus of a peptide. To identify these protons, the temperature dependence of amide NH proton chemical shifts ($\Delta\delta/\Delta T$) is typically investigated.[32,57,59] This parameter gives an insight into the type of helix formed from the pattern of H-bonding. Regular α- and 3_{10}-helices exhibit three and two free amide NH protons, respectively, at the N-terminus of a peptide, which are solvent exposed and found to be H-bonded to solvent molecules. For intramolecularly non-H-bonded, solvent exposed state, the reported temperature dependence of the amide NH proton chemical shifts ($\Delta\delta/\Delta T$) is >5.5 ppb/deg, whereas its intramolecularly H-bonded helical states have $\Delta\delta/\Delta T$ values ≤5.0 ppb/deg.[32] We found that, in contrast to its Aib (ABGY) analog under fully aqueous conditions, the L-AMV peptide shows that the $\Delta\delta/\Delta T$ values for all of its residues are <4.0 ppb/deg. Exceptions are those of the first three residues (Ala1, AMV2 and Ala3) and of the AMV6 and AMV11 residues, which differ as the Aib residues in the ABGY analog [*Supporting Information*]. In summary, in the sequence from Lys4 to Gly13 the amide NH protons appear to be in a solvent-shielded, intramolecularly H-bonded form. This result represents a clear indication of the attainment of the α-helical structure by the L-AMV peptide, unlike the case of its Aib analog where only the two N-terminal residues have $\Delta\delta/\Delta T$ values >5.5 ppb/deg but the third one has a temperature-dependent fluctuating behavior.[32] These conclusions can be authenticated by a comparison with the reported $\Delta\delta/\Delta T$ values for model rc peptides in water ($\Delta\delta/\Delta T$ ~ 7 ppb/deg)[61] and with those for a helical, 13-residue, lactam-bridged Aib-peptide in 0.1 M sodium dodecylsulphate (average $\Delta\delta/\Delta T$ ~ 2.5 ppb/deg).[29]

^{1}H NMR Spectra: Non-Sequential NOE Cross-Peaks. Non-sequential ROE/NOE cross-peaks provide valuable hints about the conformation of a peptide.[62] A considerable amount of non-sequential ROE/NOE cross-peaks was observed for the L-AMV peptide under different aqueous solvent and temperature conditions. (*Supporting Information*) The NH→NH and NH→ α/βCH regions of the 700 MHz ROE cross-peaks (mixing time: 250 ms) are discussed and highlighted in the Figures 4 and 5 below. The presence of contiguous $NH_i \rightarrow NH_{i+1}$ and $\alpha CH_i \rightarrow NH_{i+3}$ cross-peaks characterizes a regular (α- or 3_{10}-) helical backbone.[62] Furthermore, assignment of βCH→NH ROE/NOE cross-peaks can also be very useful

for the conformational analysis of peptides containing α-amino acids that lack the α-hydrogen atom (*e.g.*, AMV). Similar to $\alpha CH_i \rightarrow NH_{i+3}$, the helical signature can also be substantiated by the presence of $\beta CH_i \rightarrow NH_{i+3}$ cross-peaks along with $NH_i \rightarrow NH_{i+1}$ cross-peaks.[62]

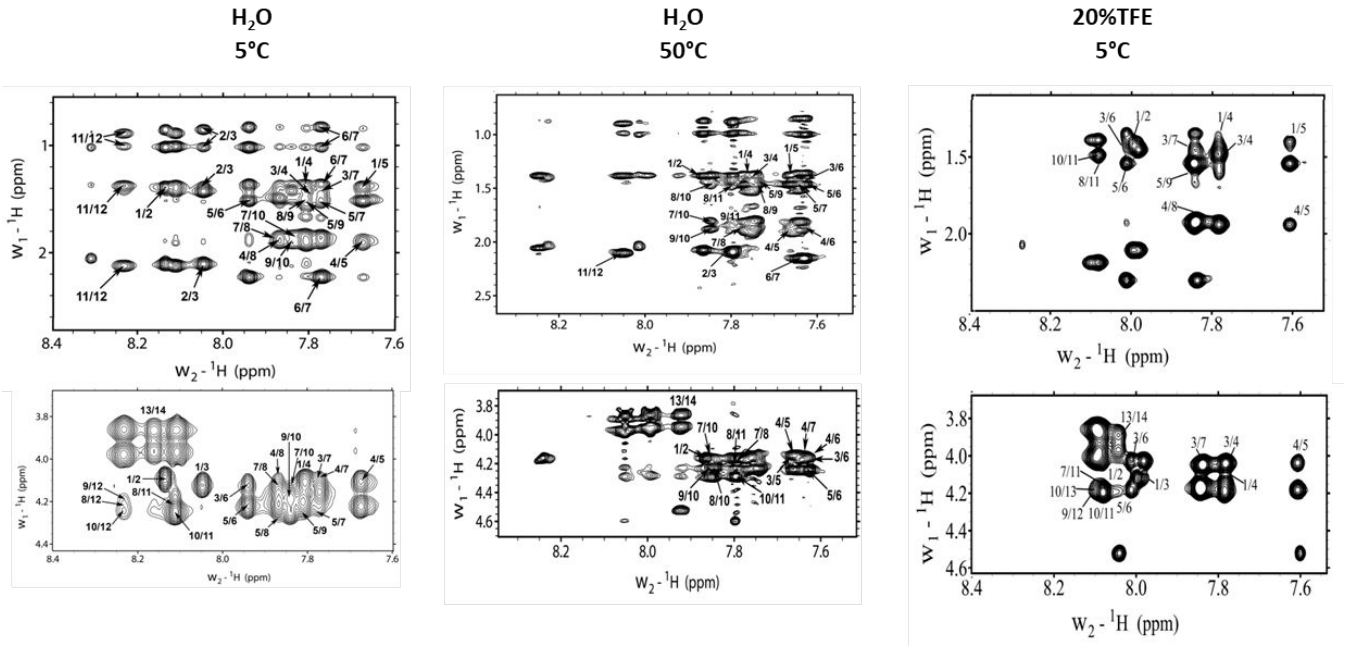

Figure 4. Regions of the ROESY spectrum of the 14-mer L-AMV peptide showing the non-sequential NOEs in H2O at 5°C and at 50°C, and in 20%TFE at 5°C. The long-range $\beta CH_i \rightarrow NH_{i+2}$, $\beta CH_i \rightarrow NH_{i+3}$, $\beta CH_i \rightarrow NH_{i+4}$ NOEs (top) and $\alpha CH_i \rightarrow NH_{i+2}$, $\alpha CH_i \rightarrow NH_{i+3}$, $\alpha CH_i \rightarrow NH_{i+4}$ NOEs (bottom) are visible.

Contiguous stretches of $NH_i \rightarrow NH_{i+1}$ cross-peaks are observed for almost all residues of L-AMV at low (5 ºC) as well as at high temperature (55 ºC) in 0% TFE (*Supplementary Information*). This result demonstrates that even at high temperature in the absence of a helicogenic agent, due to presence of the L-AMV residues in the sequence, the corresponding AMV peptide favors a helical conformation. Few $NH_i \rightarrow NH_{i+1}$ cross-peaks, which are too close to the diagonal to be resolved, are not identified unambiguously. Several $NH_i \rightarrow NH_{i+2}$ cross-peaks are also seen at low temperature for both 0% and 20% TFE/aqueous conditions. However, the number of $NH_i \rightarrow NH_{i+2}$ cross-peaks is reduced when the temperature is increased (*Supplementary Information*).

Along with the number of non-sequential $\alpha CH_i \rightarrow NH_{i+3}$ cross-peaks throughout the peptide at 5ºC under fully aqueous conditions, indicative of a helical backbone for the L-AMV peptide, a variety of $\alpha CH_i \rightarrow NH_{i+2}$ and $\alpha CH_i \rightarrow NH_{i+4}$ cross-peaks are also observed for the L-AMV peptide under different solvent and temperature conditions. The presence of $\alpha CH_i \rightarrow NH_{i+4}$ and $\beta CH_i \rightarrow NH_{i+4}$ cross-peaks, in combination with the absence of $\alpha CH_i \rightarrow NH_{i+2}$ and $\beta CH_i \rightarrow NH_{i+2}$ cross-peaks, characterizes an α-helical backbone, while for the 3_{10}-helix, the reverse is true.[16,62] In a fully aqueous state and at low temperature, the onset of a higher number of $\alpha CH_i \rightarrow NH_{i+4}$ cross-peaks (at the 3-7, 4-8, 5-9 and 8-12 positions), along with $\beta CH_i \rightarrow NH_{i+4}$ cross-peaks (at the 1-5, 3-7, 4-8 and 5-9 positions) and a very few number of $\alpha CH_i \rightarrow NH_{i+2}$ cross-peaks (only at the N- and C-termini, due to end fraying) (Figure 4) clearly confirmed the predominance of an α-helical backbone and validated the corresponding CD spectrum. However, the reverse is seen at high temperature. Although at high temperature the $\alpha CH_i \rightarrow NH_{i+4}$ cross-peaks cannot be assigned unambiguously, (due to spectral overlap), appearance of $\beta CH_i \rightarrow NH_{i+4}$ cross-peaks (at the 1-5 and 5-9 positions) together with a few $\alpha CH_i \rightarrow NH_{i+2}$ and $\beta CH_i \rightarrow NH_{i+2}$ cross-peaks (at the 4-6 and 8-10 positions) are indicative of a mixed type of helical structure (Figure 4), although the CD signature and the mean-residue ellipticity ratio point towards a predominant α-helical structure. In 20% TFE also a very few number of $\alpha CH_i \rightarrow NH_{i+4}$ and $\alpha CH_i \rightarrow NH_{i+2}$ cross-peaks is unambiguously assigned. Moreover, several $\beta CH_i \rightarrow NH_{i+2}$, $\beta CH_i \rightarrow NH_{i+3}$ and $\beta CH_i \rightarrow NH_{i+4}$ cross-peaks are noted for the peptide although all of them could not be unambiguously identified due to resonance overlap. At low temperature, the appearance of $\beta CH_i \rightarrow NH_{i+3}$ cross-peaks almost throughout the sequence in 20% TFE suggested that L-AMV peptide adopts a helical conformation. Similar cross-peaks are difficult to identify due spectral overlap when the peptide is in an aqueous state. Several $\beta CH_i \rightarrow NH_{i+4}$ cross-peaks are seen at low temperature under both full aqueous conditions and in 20% TFE, while only one $\beta CH_i \rightarrow NH_{i+2}$ cross-peak is found (between residues 5 and 7). On the other hand, at high temperature, a larger amount of $\beta CH_i \rightarrow NH_{i+2}$ cross-peaks appears compared to only two $\beta CH_i \rightarrow NH_{i+4}$ cross-peaks

(between residues 1/5 and 5/9 in 0% TFE; between residues 1-5 and 3-7 in 20% TFE). In a nutshell, from the appearance of characteristic non-sequential ROE cross-peaks, a clear consensus for the α-helical structure could be assigned to the sequence under analysis even in the absence of a helicogenic solvent. This conclusion is corroborated by considering also the R_1 and R_2 ratios obtained from the ECD spectra.

The L-AMV peptide has been also studied by ^{1}H NMR under different organic solvent and temperature conditions. In particular, these experiments have been performed in CD_3CN at 25°C and 50°C, and in CD_3OH at 25°C. The sequential $\alpha CH_i \rightarrow NH_{i+1}$ NOE signals, together with the COSY and TOCSY analyses, allow the full assignment of the spectra. A great support comes from the presence in all spectra of almost all of the sequential $NH_i \rightarrow NH_{i+1}$, that are also indicative of the onset of a helical conformation (*Supplementary Information*).

In addition, in both solvents, a number of sequential $\alpha CH_i \rightarrow NH_{i+1}$ NOEs is evident. As illustrative examples, we show the fingerprint region of the peptide in CD_3CN at 25°C and 50°C, where several $\alpha CH_i \rightarrow NH_{i+1}$ signals are clearly visible. Moreover, at the level of the AMV residues (that lack the αCH proton), $\beta CH_i \rightarrow NH_{i+1}$ NOEs are observed in all spectra (Fgure 5).

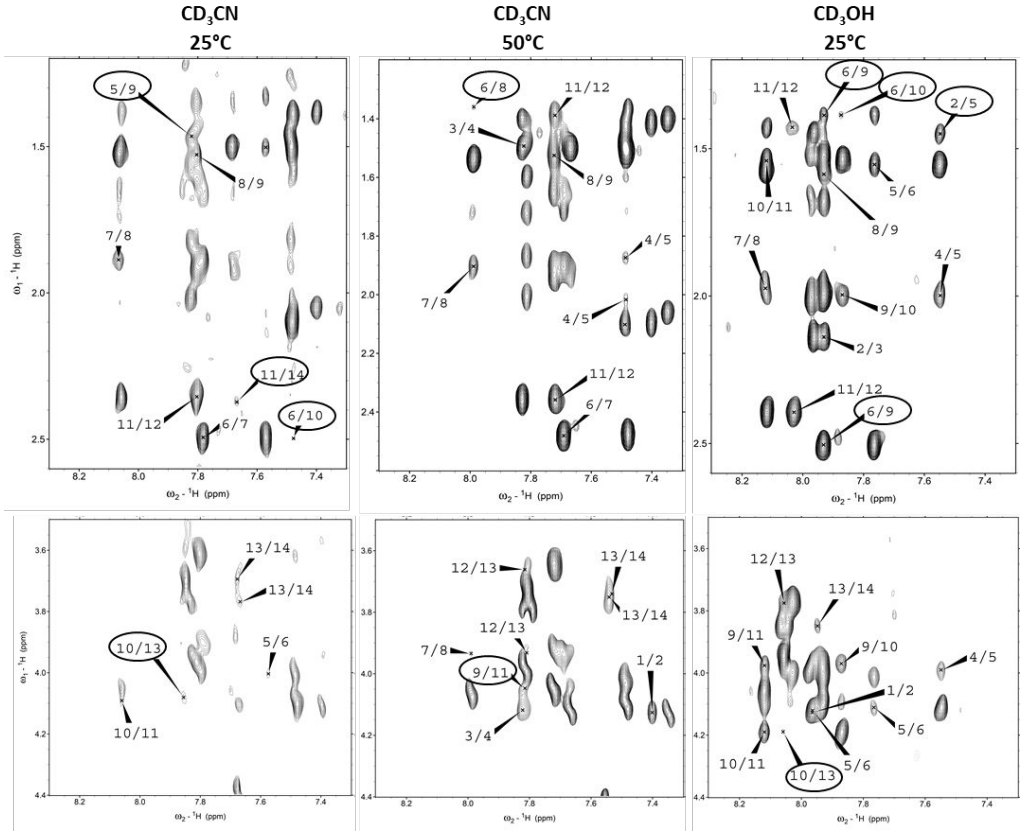

Figure 5. Regions of the ROESY spectrum of the 14-mer L-AMV peptide in CD_3CN at 25°C, in CD_3CN at 50°C, and in CD_3OH at 25°C. The long-range $\beta CH_i \rightarrow NH_{i+2}$, $\beta CH_i \rightarrow NH_{i+3}$, $\beta CH_i \rightarrow NH_{i+4}$ NOEs (top) and the long-range $\alpha CH_i \rightarrow NH_{i+2}$, $\alpha CH_i \rightarrow NH_{i+3}$, $\alpha CH_i \rightarrow NH_{i+4}$ NOEs (bottom) are highlighted with a circle.

In each CD_3CN spectrum at 25°C and 50°C, one long-range NOE suggests the presence of a helical structure. Specifically, the $\alpha CH_i \rightarrow NH_{i+3}$ (10-13) NOE is seen at 25 °C, while the $\alpha CH_i \rightarrow NH_{i+2}$ (9-11) is observed at 50°C (Figure 5, bottom). In CD_3CN at 25°C, we have evidence for the presence of the α-helical conformation as we note two $CH_i \rightarrow NH_{i+4}$ cross-peaks at the 6-10 and 5-9 positions, and two $CH_i \rightarrow NH_{i+3}$ NOEs, compatible with any of the two types of helical structure (10-13 and 11-14). In CD_3CN at 50°C, we notice a long-range $\alpha CH_i \rightarrow NH_{i+2}$ NOE (9-11) and a $\beta CH_i \rightarrow NH_{i+2}$ NOE (6-8) that are characteristic of a 3_{10}-helical conformation (Figure 5, central column).

In CD_3OH at 25°C, we observe a number of $CH_i \rightarrow NH_{i+3}$ NOEs (at the 2-5, 6-9, and 10-13 positions) and one $CH_i \rightarrow NH_{i+4}$ NOE (6-10), all compatible with the occurrence of the α-helical conformation (Figure 5, right column).

Overall, from our ^{1}H NMR study, we can reasonably conclude that the 3D-structure of the L-AMV analog is helical under all organic solvent and temperature conditions analyzed. The α-/3_{10}-helix ratio varies only a little as a function of the environment changes. In CD_3CN at 50°C our NMR results point to the co-presence of α- and 3_{10}-helices, while in CD_3CN at 25°C and in CD_3OH at 25°C, the α-helical conformation seems to largely prevail. Appearance of the 3_{10}-helical state along with the α-helical conformation in a co-existing manner especially at higher

temperature specifically emphasizes the potential role of the 3_{10}-helical state during the onset of the α-helical conformation from the statistical coil state. It should be noted that a more in-depth interpretation of these NMR data is hampered by extensive peak overlapping that will not permit any molecular dynamics calculations analysis.

CONCLUSIONS

Successful design of a thermostable, short helical peptide formed exclusively by the coded L-amino acids is really a challenging endeavor. However, incorporation of non-coded, helicogenic Aib units into the sequence indeed helps to achieve the desired target, albeit with certain limitations. Although the allowed (ϕ,ψ) main-chain torsion angles of Aib would be fully restricted in the helical region of the Ramachandran plot, due to its achiral nature an inherent, equal preference for both the right- and left-handed helical conformations is induced. Further, as Aib is able to adopt both the 3_{10}- and α-helices, peptides heavily based on Aib produces an ensemble of canonical microstates that creates a serious issue to achieve a well specific helical scaffold, *e.g.* a right-handed α-helix.

To circumvent the ambiguities arising from the incorporation of Aib, a thermally stable, water soluble, appropriate right-handed α-helical peptide model, was planned by replacing each of the three Aib units of our published 14-mer ABGY by an exceptionally effective, potentially *quasi*-rigid, helicogenic, L-configurated α-amino acid of the C^{α}-tetrasubstituted Aib class, namely C^{α}-methyl-L-valine (L-AMV), having a remarkable preference for the right-handed helical conformation. Overall, the findings in our present investigation, using complementary spectroscopic tools in aqueous as well as in organic solvents in a temperature-dependent way, clearly emphasize that our hypothesis of a multiple L-AMV inclusion is a correct decision in that the designed L-AMV containing peptide sequence not only results in an overwhelming α-helical scaffold, but also the magnitude of its helical contribution is much higher than that exhibited by its ABGY analog. Moreover, for the adoption of a predominant α-helix even under fully aqueous conditions with a pure two-state transition, our data strongly suggest that the L-AMV incorporated, water soluble, thermostable, right-handed, α-helical model peptide template would be much more appropriate to be used as a control for the experimental measurements of the thermodynamic parameters pertaining to any other amino acid, particularly to those of physiological relevance.

ASSOCIATED CONTENT

Supporting Information. MS spectrum and HPLC chromatogram of the 14-mer peptide, additional NMR data and CD deconvolution spectra. This material is available free of charge via the Internet at http://pubs.acs.org.

AUTHOR INFORMATION

Corresponding Authors

* Raja Banerjee, Department of Biotechnology, and Department of Bioinformatics, Maulana Abul Kalam Azad University of Technology, West Bengal (formerly known as West Bengal University of Technology), Salt Lake, Kolkata 700064, India; ORCID: 0000-0003-1890-6401; banraja10@gmail.com.

* Cristina Peggion, Department of Chemical Sciences, University of Padova, 35131 Padova, Italy; ORCID: 0000-0001-9716-800X; cristina.peggion@unipd.it.

Author Contributions

The manuscript was written through contributions of all authors. All authors have given approval to the final version of the manuscript.

Notes

The authors declare no competing financial interest.

ACKNOWLEDGMENT

Sincere thanks to USV Ltd., Mumbai for synthesizing the peptide; Bose Institute, Kolkata, and IISc, Bengaluru for CD facilities; Bose Institute, Kolkata for NMR facilities and Bioinformatics Lab (DBT-BIF) WBUT for the computational facilities. Swami Vivekananda Research Grant Award, WBSCST, Govt. of West Bengal (sanction no. 17.6/WBSCST/F/0530/14) and the Bioinformatics Infrastructure Facilities–Department of Biotechnology, Govt. of India [sanction no. BT/BI/25/020/2012 (BIF)] are acknowledged for their financial support. C.P. is grateful to Cariparo Foundation, Padova, for partial support to this research.

REFERENCES

(1) Anfinsen, C. B. Principles that Govern the Folding of Protein Chains. *Science* **1973**, *181* (4096), 223–230. https://doi.org/10.1126/science.181.4096.223.

(2) Chou, P. Y.; Fasman, G. D. Conformational Parameters for Amino Acids in Helical, β-Sheet, and Random Coil Regions Calculated from Proteins. *Biochemistry* **1974**, *13* (2), 211–222.

(3) Chou, P. Y.; Fasman, G. D. Prediction of the Secondary Structure of Proteins from Their Amino Acid Sequence. *Adv. Enzymol. Relat. Areas Mol. Biol.* **1978**, *47*, 45–148. https://doi.org/10.1002/9780470122921.ch2.

(4) Blout, E. R.; de Lozé, C.; Bloom, S. M.; Fasman, G. D. The Dependence of the Conformations of Synthetic Polypeptides on Amino Acid Composition. *J. Am. Chem. Soc.* **1960**, *82* (14), 3787–3789. https://doi.org/10.1021/ja01499a080.

(5) Rost, B.; Sander, C. Structure Prediction of Proteins. Where are We now? *Curr. Opin. Biotechnol.* **1994**, *5* (4), 372–380. https://doi.org/10.1016/0958-1669(94)90045-0.

(6) Rost, B.; Sander, C. Bridging the Protein Sequence-Structure Gap by Structure Predictions. *Annu. Rev. Biophys. Biomol. Struct.* **1996**, *25*, 113–136. https://doi.org/10.1146/annurev.bb.25.060196.000553.

(7) Jones, D. T. Progress in Protein Structure Prediction. *Curr. Opin. Struct. Biol.* **1997**, *7* (3), 377–387. https://doi.org/10.1016/s0959-440x(97)80055-3.

(8) Johnson, M. S.; Srinivasan, N.; Sowdhamini, R.; Blundell, T. L. Knowledge-Based Protein Modeling. *Crit. Rev.*

Biochem. Mol. Biol. **1994**, *29* (1), 1–68. https://doi.org/10.3109/10409239409086797.

(9) Ponder, J. W.; Richards, F. M. Tertiary Templates for Proteins. Use of Packing Criteria in the Enumeration of Allowed Sequences for Different Structural Classes. *J. Mol. Biol.* **1987**, *193* (4), 775–791. https://doi.org/10.1016/0022-2836(87)90358-5.

(10) Godzik, A.; Kolinski, A.; Skolnick, J. Topology Fingerprint Approach to the Inverse Protein Folding Problem. *J. Mol. Biol.* **1992**, *227* (1), 227–238. https://doi.org/10.1016/0022-2836(92)90693-e.

(11) Kamtekar, S.; Schiffer, J. M.; Xiong, H.; Babik, J. M.; Hecht, M. H. Protein Design by Binary Patterning of Polar and Nonpolar Amino Acids. *Science* **1993**, *262* (5140), 1680–1685. https://doi.org/10.1126/science.8259512.

(12) Kamtekar, S.; Hecht, M. H. Protein Motifs. 7. The Four-Helix Bundle: What Determines a Fold? *FASEB J. Off. Publ. Fed. Am. Soc. Exp. Biol.* **1995**, *9* (11), 1013–1022. https://doi.org/10.1096/fasebj.9.11.7649401.

(13) Richardson, J. S.; Richardson, D. C.; Tweedy, N. B.; Gernert, K. M.; Quinn, T. P.; Hecht, M. H.; Erickson, B. W.; Yan, Y.; McClain, R. D.; Donlan, M. E.; Surles, M. C. Looking at Proteins: Representations, Folding, Packing, and Design. *Biophys. J.* **1992**, *63* (5), 1186–1209. https://doi.org/10.1016/S0006-3495(92)81696-X.

(14) Scholtz, J. M.; Barrick, D.; York, E. J.; Stewart, J. M.; Baldwin, R. L. Urea Unfolding of Peptide Helices as a Model for Interpreting Protein Unfolding. *Proc. Natl. Acad. Sci. U. S. A.* **1995**, *92* (1), 185–189. https://doi.org/10.1073/pnas.92.1.185.

(15) Chakrabartty, A.; Baldwin, R. L. Stability of α-Helices. *Adv. Protein Chem.* **1995**, *46*, 141–176.

(16) Millhauser, G. L.; Stenland, C. J.; Hanson, P.; Bolin, K. A.; van de Ven, F. J. Estimating the Relative Populations of 3_{10}-Helix and α-Helix in Ala-Rich Peptides: a Hydrogen Exchange and High Field NMR Study. *J. Mol. Biol.* **1997**, *267* (4), 963–974. https://doi.org/10.1006/jmbi.1997.0923.

(17) Rohl, C. A.; Baldwin, R. L. Deciphering Rules of Helix Stability in Peptides. *Methods Enzymol.* **1998**, *295*, 1–26. https://doi.org/10.1016/s0076-6879(98)95032-7.

(18) Padmanabhan, S.; Jiménez, M. A.; Laurents, D. V; Rico, M. Helix-Stabilizing Nonpolar Interactions between Tyrosine and Leucine in Aqueous and TFE Solutions: 2D-1H NMR and CD Studies in Alanine-Lysine Peptides. *Biochemistry* **1998**, *37* (49), 17318–17330. https://doi.org/10.1021/bi9813678.

(19) Padmanabhan, S.; Jiménez, M. A.; Rico, M. Folding Propensities of Synthetic Peptide Fragments Covering the Entire Sequence of Phage 434 Cro Protein. *Protein Sci.* **1999**, *8* (8), 1675–1688. https://doi.org/10.1110/ps.8.8.1675.

(20) Rohl, C. A.; Chakrabartty, A.; Baldwin, R. L. Helix Propagation and N-Cap Propensities of the Amino Acids Measured in Alanine-Based Peptides in 40 Volume Percent Trifluoroethanol. *Protein Sci.* **1996**, *5* (12), 2623–2637. https://doi.org/10.1002/pro.5560051225.

(21) Chakrabartty, A.; Kortemme, T.; Baldwin, R. L. Helix Propensities of the Amino Acids Measured in Alanine-Based Peptides without Helix-Stabilizing Side-Chain Interactions. *Protein Sci.* **1994**, *3* (5), 843–852. https://doi.org/10.1002/pro.5560030514.

(22) Toniolo, C.; Bonora, G. M.; Bavoso, A.; Benedetti, E.; Di Blasio, B.; Pavone, V.; Pedone, C. Preferred Conformations of Peptides Containing α,α-Disubstituted α-Amino Acids. *Biopolymers* **1983**, *22* (1), 205–215. https://doi.org/https://doi.org/10.1002/bip.360220129.

(23) Prasad, B. V; Balaram, P. The Stereochemistry of Peptides Containing α-Aminoisobutyric Acid. *CRC Crit. Rev. Biochem.* **1984**, *16* (4), 307–348. https://doi.org/10.3109/10409238409108718.

(24) Balaram, P. The Design and Construction of Synthetic Protein Mimics. *Pure Appl. Chem.* **1992**, *64* (8), 1061–1066. https://doi.org/10.1351/pac199264081061.

(25) Schweitzer-Stenner, R.; Gonzales, W.; Bourne, G. T.; Feng, J. A.; Marshall, G. R. Conformational Manifold of α-Aminoisobutyric Acid (Aib) Containing Alanine-Based Tripeptides in Aqueous Solution Explored by Vibrational Spectroscopy, Electronic Circular Dichroism Spectroscopy, and Molecular Dynamics Simulations. *J. Am. Chem. Soc.* **2007**, *129* (43), 13095–13109. https://doi.org/10.1021/ja0738430.

(26) Karle, I. L.; Balaram, P. Structural Characteristics of α-Helical Peptide Molecules Containing Aib Residues. *Biochemistry* **1990**, *29* (29), 6747–6756. https://doi.org/10.1021/bi00481a001.

(27) Marshall, G. R.; Hodgkin, E. E.; Langs, D. A.; Smith, G. D.; Zabrocki, J.; Leplawy, M. T. Factors Governing Helical Preference of Peptides Containing Multiple α,α-Dialkyl Amino Acids. *Proc. Natl. Acad. Sci. U. S. A.* **1990**, *87* (1), 487–491. https://doi.org/10.1073/pnas.87.1.487.

(28) Banerjee, R.; Basu, G.; Chène, P.; Roy, S. Aib-Based Peptide Backbone as Scaffolds for Helical Peptide Mimics. *J. Pept. Res.* **2002**, *60* (2), 88–94.

(29) Schievano, E.; Bisello, A.; Chorev, M.; Bisol, A.; Mammi, S.; Peggion, E. Aib-Rich Peptides Containing Lactam-Bridged Side Chains as Models of the 3_{10}-Helix. *J. Am. Chem. Soc.* **2001**, *123* (12), 2743–2751. https://doi.org/10.1021/ja0027261.

(30) Banerjee, R.; Basu, G. Direct Evidence for Alteration of Unfolding Profile of a Helical Peptide by far-Ultraviolet Circular Dichroism Aromatic Side-Chain Contributions. *FEBS Lett.* **2002**, *523* (1–3), 152–156.

(31) Banerjee, R.; Basu, G. A Short Aib/Ala-Based Peptide Helix is as Stable as an Ala-Based Peptide Helix Double Its Length. *ChemBioChem* **2002**, *3* (12), 1263–1266. https://doi.org/10.1002/1439-7633(20021202)3:12<1263::AID-CBIC1263>3.0.CO;2-O.

(32) Banerjee, R.; Chattopadhyay, S.; Basu, G. Conformational Preferences of a Short Aib/Ala-Based Water-Soluble Peptide as a Function of Temperature. *Proteins* **2009**, *76* (1), 184–200. https://doi.org/10.1002/prot.22337.

(33) Karle, I. L.; Flippen-Anderson, J. L.; Gurunath, R.; Balaram, P. Facile Transition between 3_{10}- and α-Helix: Structures of 8-, 9-, and 10-Residue Peptides Containing the -(Leu-Aib-Ala)$_2$-Phe-Aib- Fragment. *Protein Sci.* **1994**, *3* (9), 1547–1555. https://doi.org/10.1002/pro.5560030920.

(34) Basu, G.; Kuki, A. Conformational Preferences of Oligopeptides Rich in α-Aminoisobutyric Acid. II. A Model for the 3_{10}-/α-Helix Transition with Composition and Sequence Sensitivity. *Biopolymers* **1992**, *32* (1), 61–71. https://doi.org/10.1002/bip.360320109.

(35) Toniolo, C.; Benedetti, E. The Polypeptide 3_{10}-Helix. *Trends Biochem. Sci.* **1991**, *16* (9), 350–353.

(36) Pace, C. N. Determination and Analysis of Urea and Guanidine Hydrochloride Denaturation Curves. *Methods Enzymol.* **1986**, *131*, 266–280. https://doi.org/10.1016/0076-6879(86)31045-0.

(37) Shenkarev, Z. O.; Paramonov, A. S.; Nadezhdin, K. D.; Bocharov, E. V; Kudelina, I. A.; Skladnev, D. A.; Tagaev, A. A.; Yakimenko, Z. A.; Ovchinnikova, T. V; Arseniev, A. S. Antiamoebin I in Methanol Solution: Rapid Exchange between Right-Handed and Left-Handed 3(10)-Helical Conformations. *Chem. Biodivers.* **2007**, *4* (6), 1219–1242. https://doi.org/10.1002/cbdv.200790106.

(38) Hummel, R.-P.; Toniolo, C.; Jung, G. Conformational Transitions between Enantiomeric 3(10)-Helices. *Angew. Chem. Int. Ed.* **1987**, *26* (11), 1150–1152. https://doi.org/https://doi.org/10.1002/anie.198711501.

(39) Kubasik, M.; Kotz, J.; Szabo, C.; Furlong, T.; Stace, J. Helix-Helix Interconversion Rates of Short 13C-Labeled Helical Peptides as Measured by Dynamic NMR Spectroscopy. *Biopolymers* **2005**, *78* (2), 87–95. https://doi.org/10.1002/bip.20235.

(40) Manning, M. C.; Woody, R. W. Theoretical CD Studies of Polypeptide Helices: Examination of Important Electronic and Geometric Factors. *Biopolymers* **1991**, *31* (5), 569–586. https://doi.org/10.1002/bip.360310511.

(41) Yang, J. T.; Wu, C.-S. C.; Martinez, H. M. Calculation of Protein Conformation from Circular Dichroism. *Methods Enzymol.* **1986**, *130*, 208–269.

(42) Greenfield, N. J.; Fasman, G. D. Computed Circular Dichroism Spectra for the Evaluation of Protein Conformation. *Biochemistry* **1969**, *8* (10), 4108–4116.

(43) Toniolo, C.; Polese, A.; Formaggio, F.; Crisma, M.; Kamphuis, J. Circular Dichroism Spectrum of a Peptide 3(10)-Helix. *J. Am. Chem. Soc.* **1996**, *118* (11), 2744–2745. https://doi.org/10.1021/ja9537383.

(44) Banerjee, R.; Sheet, T. Ratio of Ellipticities between 192 and 208 nm (R_1): an Effective Electronic Circular Dichroism Parameter for Characterization of the Helical Components of Proteins and Peptides. *Proteins Struct. Funct. Bioinformat.* **2017**, *85* (11), 1975–1982. https://doi.org/10.1002/prot.25351.

(45) Crisma, M.; Toniolo, C. Helical Screw-Sense Preferences of Peptides Based on Chiral, C^{α}-Tetrasubstituted α-Amino Acids. *Biopolymers* **2015**, *104* (1), 46–64. https://doi.org/10.1002/bip.22581.

(46) Polese, A.; Formaggio, F.; Crisma, M.; Valle, G.; Toniolo, C.; Bonora, G. M.; Broxterman, Q. B.; Kamphuis, J. Peptide Helices as Rigid Molecular Rulers: a Conformational Study of Isotactic Homopeptides from α-Methyl-α-Isopropylglycine, [L-(αMe)Val]. *Chem. – A Eur. J.* **1996**, *2* (9), 1104–1111.
https://doi.org/https://doi.org/10.1002/chem.19960020911.

(47) Atherton, E.; Sheppard R.C., Solid-Phase Peptide Synthesis using Nα-Fluorenylmethoxycarbonyl Amino Acid Pentafluorophenyl Esters. J. *Chem. Soc., Chem. Comm.* **1985** (3) 165-166. https://doi.org/10.1039/C39850000165.

(48) Carpino, L. A.; Han, G. Y. 9-Fluorenylmethoxycarbonyl Function, a New Base-Sensitive Amino-Protecting Group. *J. Am. Chem. Soc.* **1970**, *92* (19), 5748–5749. https://doi.org/10.1021/ja00722a043.

(49) Miles, A. J.; Wallace, B. A. CDtoolX, a Downloadable Software Package for Processing and Analyses of Circular Dichroism Spectroscopic Data. *Protein Sci.* **2018**, *27* (9), 1717–1722. https://doi.org/10.1002/pro.3474.

(50) Roberts, G. C. K. *NMR of Macromolecules: A Practical Approach*; Roberts, G. C. K., Ed.; IRL Press, 1993.

(51) Goddard, T. D.; Knelle, D. G. Sparky 3. University of California, San Francisco, 2007.

(52) Bruch, M. D.; Dhingra, M. M.; Gierasch, L. M. Side Chain-Backbone Hydrogen Bonding Contributes to Helix Stability in Peptides Derived from an α-Helical Region of Carboxypeptidase A. *Proteins* **1991**, *10* (2), 130–139. https://doi.org/10.1002/prot.340100206.

(53) Andersen, N. H.; Liu, Z.; Prickett, K. S. Efforts toward Deriving the CD Spectrum of a 3_{10}- Helix in Aqueous Medium. *FEBS Lett.* **1996**, *399* (1–2), 47–52. https://doi.org/10.1016/S0014-5793(96)01279-3.

(54) Yokum, T. S.; Gauthier, T. J.; Hammer, R. P.; McLaughlin, M. L. Solvent Effects on the 3_{10}-/α-Helix Equilibrium in Short Amphipathic Peptides Rich in α,α-Disubstituted Amino Acids. *J. Am. Chem. Soc.* **1997**, *119* (5), 1167–1168. https://doi.org/10.1021/ja962875c.

(55) Sudha, T. S.; Vijayakumar, E. K. S.; Balaram, P. Circular Dichroism Studies of Helical Oligopeptides: Can 3_{10}- and α-Helical Conformations be Chiroptically Distinguished? *Int. J. Pept. Protein Res.* **1983**, *22* (4), 464–468. https://doi.org/10.1111/j.1399-3011.1983.tb02116.x.

(56) Woody, R. W. Circular Dichroism of Peptides. In *Conformation in Biology and Drug Design*; Udenfriend, S., Meienhofer, J., Hruby, V. J., Eds.; Academic Press, 1985; pp 15–114. https://doi.org/10.1016/B978-0-12-304207-1.50008-4.

(57) Wishart, D. S.; Sykes, B. D. Chemical Shifts as a Tool for Structure Determination. *Methods Enzymol.* **1994**, *239*, 363–392.

(58) Bundi, A.; Wüthrich, K. 1H-NMR Parameters of the Common Amino Acid Residues Measured in Aqueous Solutions of the Linear Tetrapeptides H-Gly-Gly-X-L-Ala-OH. *Biopolymers* **1979**, *18* (2), 285–297. https://doi.org/10.1002/bip.1979.360180206.

(59) Avbelj, F.; Kocjan, D.; Baldwin, R. L. Protein Chemical Shifts Arising from α-Helices and β-Sheets Depend on Solvent Exposure. *Proc. Natl. Acad. Sci. U. S. A.* **2004**, *101* (50), 17394–17397. https://doi.org/10.1073/pnas.0407969101.

(60) Smith, L. J.; Bolin, K. A.; Schwalbe, H.; MacArthur, M. W.; Thornton, J. M.; Dobson, C. M. Analysis of Main Chain Torsion Angles in Proteins: Prediction of NMR Coupling Constants for Native and Random Coil Conformations. *J. Mol. Biol.* **1996**, *255* (3), 494–506. https://doi.org/10.1006/jmbi.1996.0041.

(61) Merutka, G.; Dyson, J. H.; Wright, P. E. 'Random Coil' 1H Chemical Shifts Obtained as a Function of Temperature and Trifluoroethanol Concentration for the Peptide Series GGXGG. *J. Biomol. NMR* **1995**, *5* (1), 14–24. https://doi.org/10.1007/BF00227466.

(62) Wüthrich, K. *NMR of Proteins and Nucleic Acids.*; John Wiley and Sons, New York, 1986.

TOC.

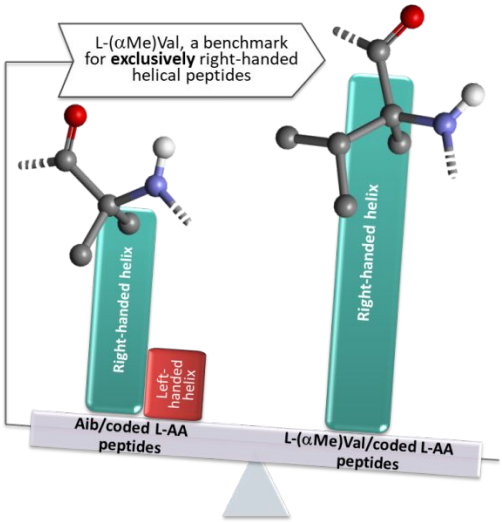
L-(αMe)Val, a benchmark for **exclusively** right-handed helical peptides
Right-handed helix
Left-handed helix
Right-handed helix
Aib/coded L-AA peptides
L-(αMe)Val/coded L-AA peptides